Contents lists available at Science-Gate

International Journal of Advanced and Applied Sciences

Journal homepage: http://www.science-gate.com/IJAAS.html

Therapeutic potential of *Moringa oleifera*-derived isothiocyanates: Targeting adenosine A_1 receptors in heart failure management

Roaa M. Alreemi *

Department of Biochemistry, College of Science, University of Jeddah, Jeddah, Saudi Arabia

ARTICLE INFO

Article history:
Received 13 October 2024
Received in revised form
12 February 2025
Accepted 11 July 2025

Keywords:
Isothiocyanates
Moringa oleifera
Adenosine A_1 receptor
Molecular docking
Therapeutic potential

ABSTRACT

Isothiocyanates (ITCs) are bioactive compounds found in various plants, including *Moringa oleifera*, and are known for their health benefits, such as anticancer and anti-inflammatory effects. This study examines the interactions between four *Moringa oleifera*-derived isothiocyanates (MITCs) and adenosine A_1 receptors (A_1R), which are important in cardiovascular, neurological, and other physiological functions. The SuperPred server was used for target prediction and confirmed a high binding probability of all MITC derivatives with A_1R. Molecular docking analysis identified MITC-1 as the most promising compound based on its strong binding score. Further molecular dynamics (MD) simulations over 100 nanoseconds showed that the MITC-1–A_1R complex had high binding affinity and remained stable, suggesting its potential as an A_1R antagonist. Additionally, ADMET analysis indicated favorable drug-like properties for these compounds. These findings highlight the therapeutic potential of *Moringa oleifera*-derived ITCs in treating heart failure and other A_1R-related disorders, providing a basis for future laboratory and clinical research.

1. Introduction

Isothiocyanates (ITCs) are a diverse group of sulfur-containing phytochemicals renowned for their wide range of health benefits. Found predominantly in plants of the Brassicaceae family, such as broccoli, cauliflower, cabbage, Brussels sprouts, and mustard seeds. These compounds are produced through the hydrolysis of glucosinolates by the enzyme myrosinase. This process occurs as a defense mechanism against herbivores and pathogens or upon physical damage to plant tissues (Mastuo et al., 2020; Na et al., 2023; Olayanju et al., 2024). Structurally, ITCs consist of a carbon-nitrogen double bond (–N=C=S) attached to an aryl or alkyl group, and variations in their side chains influence their biological properties and activities. ITCs have been extensively studied for their therapeutic potential, demonstrating anticancer, antioxidant, anti-inflammatory, and anti-diabetic effects (Mastuo et al., 2020; Na et al., 2023; Sahin et al., 2019). Additionally, they show promise in the prevention of cardiovascular and neurodegenerative diseases (Giacoppo et al., 2015; Kamal et al., 2022; Olayanju et al., 2024).

Although *Moringa oleifera* (*M. oleifera*) does not belong to the Brassicaceae family, it is nonetheless a rich source of isothiocyanates (ITCs), which often exhibit distinct structural features compared to those found in Brassicaceae species. These ITCs are typically glycosylated, meaning they have one or more sugar moieties attached, which influences their stability, solubility, interaction with biological targets, and overall metabolism. Such glycosylation can lead to unique biological effects and health benefits (Lopez-Rodriguez et al., 2020; Waterman et al., 2014).

The primary ITCs isolated from M. oleifera include compound 1 (glucosylated benzyl isothiocyanate), compound 2 (acetylated rhamnosyl benzyl isothiocyanate), and two hydroxylated phenoxy derivatives (compounds 3 and 4) as shown in Table 1 (Fig. 1; Jaja-Chimedza et al., 2017; Olayanju et al., 2024; Waterman et al., 2014).

The adenosine receptors are a group of G protein-coupled receptors (GPCRs) that respond to adenosine. These receptors are involved in a wide range of physiological processes, including heart rate regulation, immune response, tissue repair, and cellular proliferation. There are four primary subtypes of adenosine receptors, including A_1R, $A_{2A}R$, $A_{2B}R$, and A_3R, and each subtype has distinct

* Corresponding Author.
Email Address: rmalreemi@uj.edu.sa
https://doi.org/10.21833/ijaas.2025.08.009
Corresponding author's ORCID profile:
https://orcid.org/0000-0002-9062-5674

roles and mechanisms of action that impact physiological and pathological processes due to their widespread distribution across the body (Borea et al., 2018; Sheth et al., 2014; Vincenzi et al., 2023). Adenosine A_1 receptor (A_1R) is one of these subtypes that mediate the diverse effects of adenosine. A_1R plays a crucial role in various physiological functions due to its widespread presence in the brain and other peripheral tissues, such as the heart, kidneys, and lungs. A_1R receptor is involved in regulating cardiovascular, renal, and central nervous system functions. It mediates significant processes such as heart rate regulation, neuroprotection, sleep-wake cycles, and vasodilation (Basheer et al., 2004; Nguyen et al., 2023; Tawfik et al., 2005). A_1R also plays a significant role in renal function by modulating the glomerular filtration rate (Dhalla et al., 2003; Nguyen et al., 2023; Vallon et al., 2008).

A_1R reduces heart rate and myocardial contractility by lowering cAMP and calcium influx, conserving energy under normal conditions. However, excessive activation exacerbates congestive heart failure (CHF) by causing bradycardia and reduced cardiac output. A_1R antagonists improve CHF by boosting contractility, heart rate, and promoting diuresis to alleviate fluid retention. This study aims to explore *Moringa oleifera*-derived isothiocyanates as potential A_1R modulators to enhance heart failure management strategies.

Table 1: Common isothiocyanates (ITCs) found in *Moringa oleifera* leaves

Compound	Name
1	4-(α-L-rhamnosyloxy)-benzyl isothiocyanate
2	4-[(4′-O-acetyl-α-L-rhamnosyloxy)benzyl]isothiocyanate
3	[3,5-dihydroxy-2-[4-(isothiocyanatomethyl)phenoxy]-6-methyloxan-4-yl] acetate
4	[4,5-dihydroxy-2-[4-(isothiocyanatomethyl)phenoxy]-6-methyloxan-3-yl] acetate

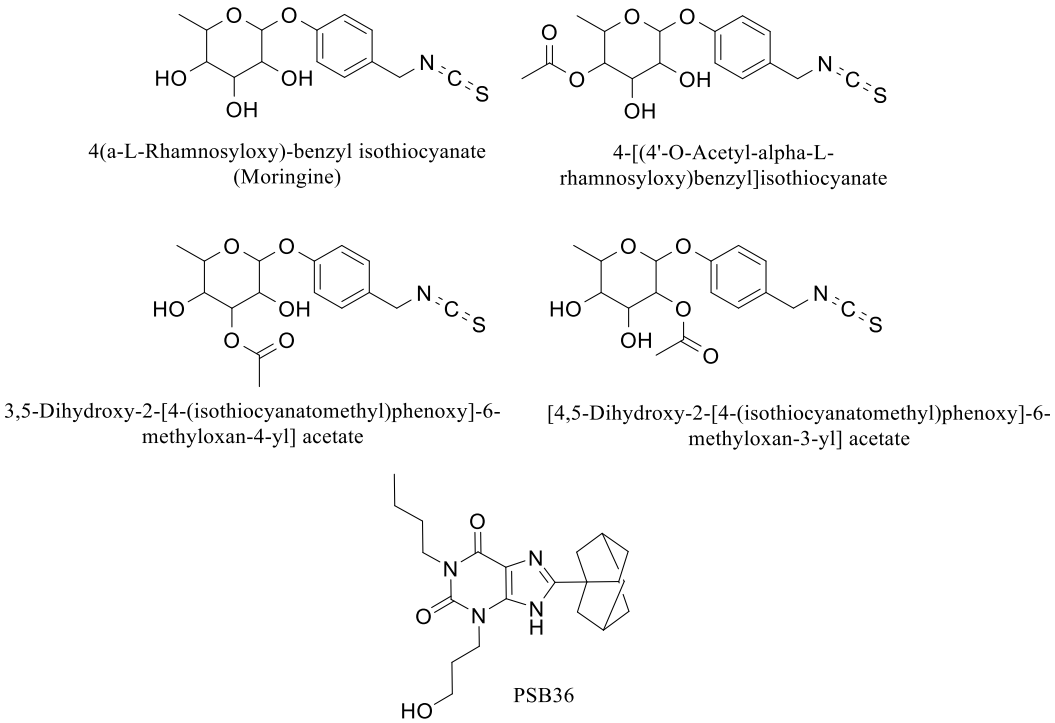

Fig. 1: The chemical structures of the *M. oleifera*-derived ITCs derivatives and the co-crystallized ligand (PDB ID: 5N2S)

2. Materials and methods

2.1. Target prediction

SuperPred server is used to predict potential targets and therapeutic uses of ITCs from *M. oleifera* based on their structural similarity to existing drugs. SuperPred leverages machine learning to compare the structural fingerprints of compounds under study with those of known, approved drugs. If the compound structure is similar to those of approved drugs, SuperPred predicts the Anatomical Therapeutic Chemical (ATC) code(s) and potential therapeutic target(s) for the compound (Dunkel et al., 2008). After the target prediction, the probability score and the model accuracy score were reported. Where the probability score indicates the likelihood that the investigated compound will bind to a specific predicted target, and the model accuracy score reflects the prediction accuracy for specific targets within the SuperPred model (Dunkel et al., 2008). The target common for all ITCs from *M. oleifera* (MITCs) was used for molecular docking and further studies.

2.2. Protein preparation

The crystal structure of adenosine A_1 receptors (A_1R) (PDB: 5N2S) was prepared with the Protein Preparation Wizard in the Schrödinger suite (Schrödinger, 2024c). This preparation included adding hydrogen atoms to residues and removing

water molecules located more than 5 Å from the protein. The protonation states of residues were generated using Epik, and the charges on metal ions were adjusted. Further refinement was achieved by predicting the pKa values of ionizable residues with PROPKA. The process concluded with restrained minimization of the protein using the OPLS4 force field.

2.3. Ligand preparation

Ligand preparation is a crucial initial step in molecular docking studies, ensuring that ligands are accurately represented and ready to interact with target proteins. In this study, the LigPrep module from the Schrödinger suite was employed to prepare MITCs (Schrödinger, 2024b). The 2D structures of the ligands were converted to 3D and energy-minimized using the OPLS3 force field. LigPrep also maintained ionization states and generated all possible tautomers and ionized forms. Additionally, Epik was used to create these forms at pH 7.0±0.2, with the desalt option selected. Hydrogen bonds were optimized by predicting the pKa of ionizable groups using PROPKA. This comprehensive preparation ensures that all potential forms of the ligands are considered during the docking process.

2.4. Grid generation and molecular docking

A grid box was created around the co-crystallized ligand PSB36 in the protein crystal structure (PDB: 5N2S) using Glide's Receptor-Grid-Generation tool (Schrödinger, 2024a). Docking of the MITCs was carried out within this grid box. The VdW radii scaling factor for nonpolar atoms was set to 1.0, and the partial charge cutoff was 0.25. Docking was executed using the Ligand Docking tool of Schrödinger, employing the extra precision (XP) protocol (Schrödinger, 2024a). All other parameters were left in their default settings. To assess the docking method, re-docking of the co-crystallized ligand (PDB: 5N2S) was conducted before docking the MITCs.

2.5. Molecular simulation

After reviewing the ligand interaction diagrams, the top MITC, based on docking scores, was selected for molecular dynamics (MD) simulation. The MD simulations were conducted using the Desmond package from the Schrödinger suite to assess the effectiveness of the compounds identified through docking. The TIP3P solvent model was employed with an orthorhombic box of 10 Å dimensions. Sodium ions were added to neutralize the system. The OPLS4 force field was used for energy minimization, which involved heating and equilibrating the complex prior to the MD production phase. The initial energy minimization was performed with the steepest descent method, followed by heating from 0 to 300 K. During the 100 ns simulation, the protein-ligand complexes were evaluated at pH 7.0±0.2, with the system maintained at 300 K and 1.01325 atm pressure using an NPT ensemble.

2.6. Prediction of ADMET properties

The drug-like and the absorption, distribution, metabolism, excretion, and toxicity (ADMET) properties of MITCs were evaluated using the QikProp module in Schrödinger (Ioakimidis et al., 2008; Schrödinger, 2024d). The model efficiently identified various descriptors. The predicted values are compared against the recommended ranges established from the values observed in 95% of known drugs.

3. Results and discussion

3.1. Target prediction process

The process of identifying suitable targets to evaluate the therabiotic effects of ITCs from *M. oleifera* (MITCs) involved using ligand-based target prediction methods. The SuperPred web server was employed to determine the ATC (anatomical therapeutic chemical) codes and to forecast potential targets for the MITCs. Based on the analysis of the predicted target proteins, the adenosine A_1 receptor (A_1R) was chosen for further investigation due to its high probability and model accuracy (Table 2). The crystal structure of the human A_1R receptor (PDB ID: 5N2S) (Cheng et al., 2017) was utilized, complexed with the selective antagonist 1-butyl-3-(3-hydroxypropyl)-8-(3-noradamantyl) xanthine (PSB36), which is employed to investigate A_1R receptor-mediated cell signaling. After identifying the target and selecting the corresponding crystal structure, the MITCs were docked into the protein structure.

3.2. Ligands, protein preparation, and molecular docking

After preparing the protein and ligands, the ligands' 3D structures were docked into the designated grid box within the A_1R receptor binding pocket (PDB-ID: 5N2S) that was prepared using the Receptor Grid Generation tool from Glide in Maestro. The native ligand PSB36 was also docked into the co-crystallized binding site of the A_1R receptor. Docking scores, Glide GScore, Glide Emodel, and XP GScore, were calculated and are summarized in Table 3. MITC-1 demonstrated enhanced binding to the A_1R receptor with a docking score of -7.470 kcal/mol, compared to the native ligand PSB36, which had a docking score of -11.978 kcal/mol. The docking scores indicated that MITC-1 exhibited a favorable binding conformation and relative affinity to the receptor. For validation of the docking procedure, the native ligand PSB36 was redocked, and the docking poses were compared to the original pose of

PSB36 in the crystal structure, yielding an RMSD of 1.033 (Fig. 2).

The xanthine part of the native ligand PSB36 forms two π–π stacking interactions with PHE-1276. In addition, its amino and carbonyl groups form two hydrogen bonds with ASN-1359. The hydroxyl group on the side chain also forms a hydrogen bond with HIS-1383 (Fig. 3).

Table 2: Predicted target probability and model accuracy for MITCs against A_1R receptors using the SuperPred web server

ITCs	Probability*	Model accuracy**
MITC-1	91.89%	95.93%
MITC-2	81.71%	95.93%
MITC-3	87.12%	95.93%
MITC-4	88.74%	95.93%

*: The probability of MITCs binding to a particular target was assessed using the corresponding target-specific machine learning model; **: The accuracy of the prediction model is indicated by a 10-fold cross-validation score of the logistic regression model, highlighting performance variability across different targets

In the case of MITC-1, the benzene ring forms one π–π stacking interaction with PHE-1276. The pyran ring forms a hydrogen bond with ASN-1359, and the isothiocyanate group forms another hydrogen bond with HIS-1383 (Fig. 4). Both PSB36 and MITC-1 bind to the same amino acid residues at the binding site, but with a different number of interactions. The native ligand (PSB36) forms three hydrogen bonds and two π–π stacking interactions, whereas MITC-1 forms two hydrogen bonds and one π–π stacking interaction. This difference explains the lower docking score of MITC-1 compared to PSB36.

Despite the lower docking score, MITC-1 still showed a notable binding affinity. Therefore, MD simulation was carried out to further investigate the protein–ligand interaction.

Table 3: Docking scores of MITCs and co-crystallized ligand PSB36 with A_1R receptor (PDB: 5N2S)

	Docking score	Glide gscore	Glide emodel	XP GScore
PSB36	-11.978	-12.03	-74.494	-12.03
MITC-1	-7.47	-8.528	-53.998	-8.528
MITC-4	-7.397	-8.45	-56.41	-8.45
MITC-3	-6.946	-7.056	-56.24	-7.056
MITC-2	-5.44	-5.549	-48.779	-5.549

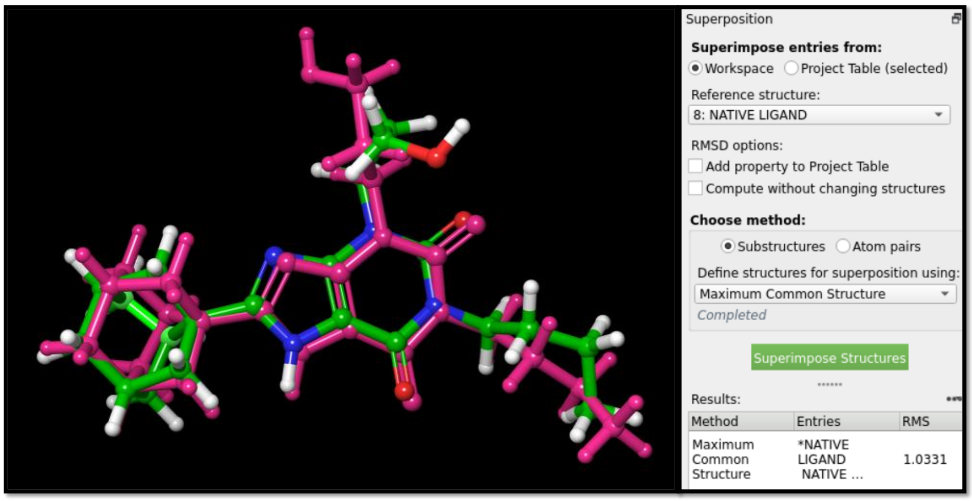

Fig. 2: The 3D structure of the re-docked native ligand PSB36 (pink) superimposed on the co-crystallized ligand PSB36 (green)

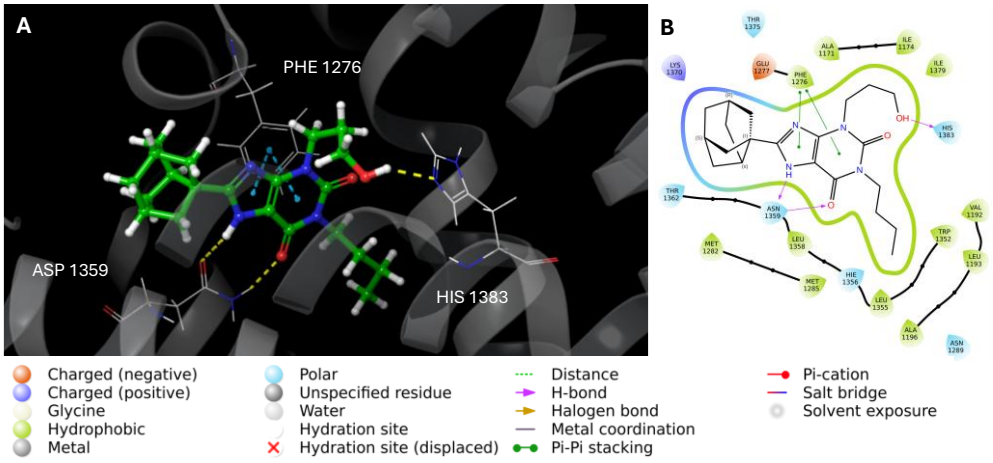

Fig. 3: (A) The 3D ligand interaction diagram of PSB36 with A_1R receptor (PDB: 5N2S). (B) 2D depiction of the protein-ligand interactions

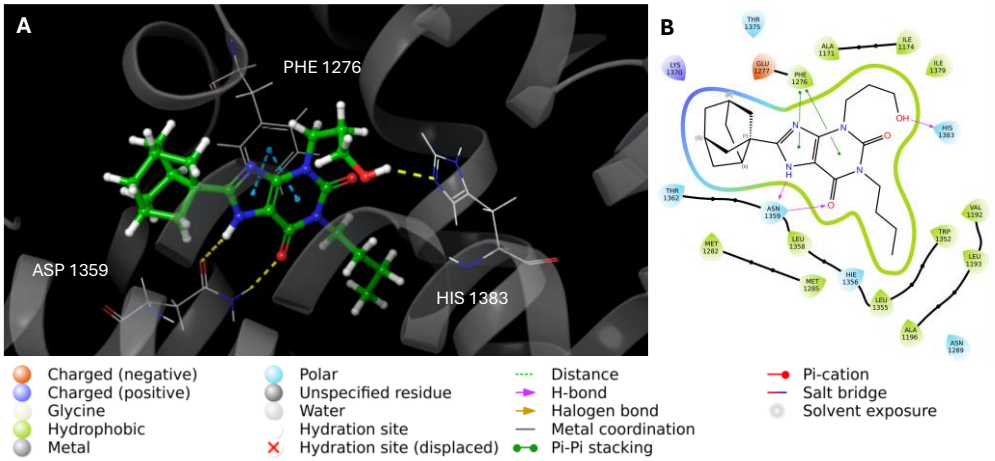

Fig. 4: (A) The 3D ligand interaction diagram of MITC-1 with A_1R receptor (PDB: 5N2S). (B) 2D depiction of the protein-ligand interactions

3.3. MD simulation

Molecular dynamics (MD) simulations were carried out using Desmond software to recreate the aqueous physiological environment and examine changes in protein conformation and binding affinity over a nanosecond timescale, relative to the original affinity and conformation observed in the crystal structure. The study concentrated specifically on the highest docking scoring MITCs from the docking analysis (MITC-1) along with the reference ligand PSB36.

Fig. 5 represents the binding affinity and stability of the protein-ligand complex during the simulation period. The root mean square deviation (RMSD) is a calculated metric used to compare the poses of the MITC-1 to that of the co-crystallized ligand. RMSD plots for the ligands complexed with protein measure the average positional changes of the atoms in both the protein and ligand within the binding pocket at the end of the 100 ns simulation, relative to their initial positions at 0 ns. The RMSD of A_1R receptor complexed with both PSB36 and MITC-1 showed slight fluctuations beyond the acceptable range, up to 4 Å. This suggests that the protein is somewhat unstable and experienced conformational changes during the simulation (Figs. 5A, 5B). The RMSD plot for both PSB36 and MITC-1 indicated ligand stability with minor fluctuations remaining insignificant, falling within the acceptable range of 1–3 Å (Figs. 5A, 5B). Both PSB36 and MITC-1 showed fluctuation in the plots observed during the initial period of the simulation, as seen in Fig. 5, within the first 25 ns. This anticipated variation occurs as the compounds continuously adjust their conformation within the binding pocket to achieve a pose that minimizes free energy.

The ligand's interactions with the amino acid residues of the protein binding pocket can be monitored throughout the simulation. These interactions can be classified and summarized by type, as shown in Fig. 6 and Fig. 7. Stacked bar charts that are color-coded based on the interaction types, including hydrogen bonds, hydrophobic interactions, and water bridges. The stacked bar chart and the 2D schematic diagram of the co-crystallized ligand complexed with A_1R showed two hydrogen interactions between the xanthine moiety of the ligand and ASN-1359 residue of the receptor that were maintained for 100% and 99% of simulation time. Other key interactions, including the hydrophobic interaction of the ligand pyrimidine ring of xanthine with PHE-1276 (76%) and the water bridge of the hydroxyl group with ALA-1171, continued for 47% of simulation time (Figs. 6A, 6B). The top panel of Fig. 6C illustrates the overall specific interactions between the co-crystallized ligand and the protein. The bottom panel highlights the protein residues that interact with the ligand at various time points. The dark orange color in the bottom panel was observed with several residues throughout the trajectory, including ASN-1359, PHE1276, and ALA-1171, which indicate the prolonged binding and high stability of protein and ligand interaction (Fig. 6C).

2D schematic diagram and the stacked bar chart and in Figs. 7A and 7B displayed the interaction of MITC-1 with A_1R receptor residues that continued for more than 30% of the simulation duration. The hydroxyl groups of the pyran ring in the ligand form hydrogen bonds with Thr1375 and three water bridges with ILE-1280, LEU1359, and THR-1362 that were maintained for 84%, 65%, 75%, and 82% of simulation time, respectively. Furthermore, the oxygen of pyran interacts via a hydrogen bond with ASG-1359 for 96% of the simulation period. The top panel of Fig. 7C illustrates the total specific interactions between MITC-1 and the A_1R receptor. The bottom panel details the protein residues that interacted with the ligand at each time point. The dark orange coloration in the bottom panel indicates multiple residues engaged with the ligand throughout the trajectory, including PHE-1276, ILE-1280, LEU-1358, ASN-1359, THR-1362, and THR-1375 (Fig. 7C).

The comparative analysis of molecular dynamic simulation revealed that MITC-1 had a higher number of binding interactions (Fig. 7C) compared to the native ligand (Fig. 6C). This difference is attributed to the structural variations and the three-

dimensional conformation within the binding pocket and the number of interactions. However, the variations in the result of docking and molecular dynamics simulation are due to several reasons. Where docking typically treats the protein and ligand as rigid, providing a static snapshot of binding interactions and estimating affinity using simplified scoring functions. In contrast, MD simulations account for the full flexibility of molecules, environmental factors such as solvent effects, and dynamic behavior over time.

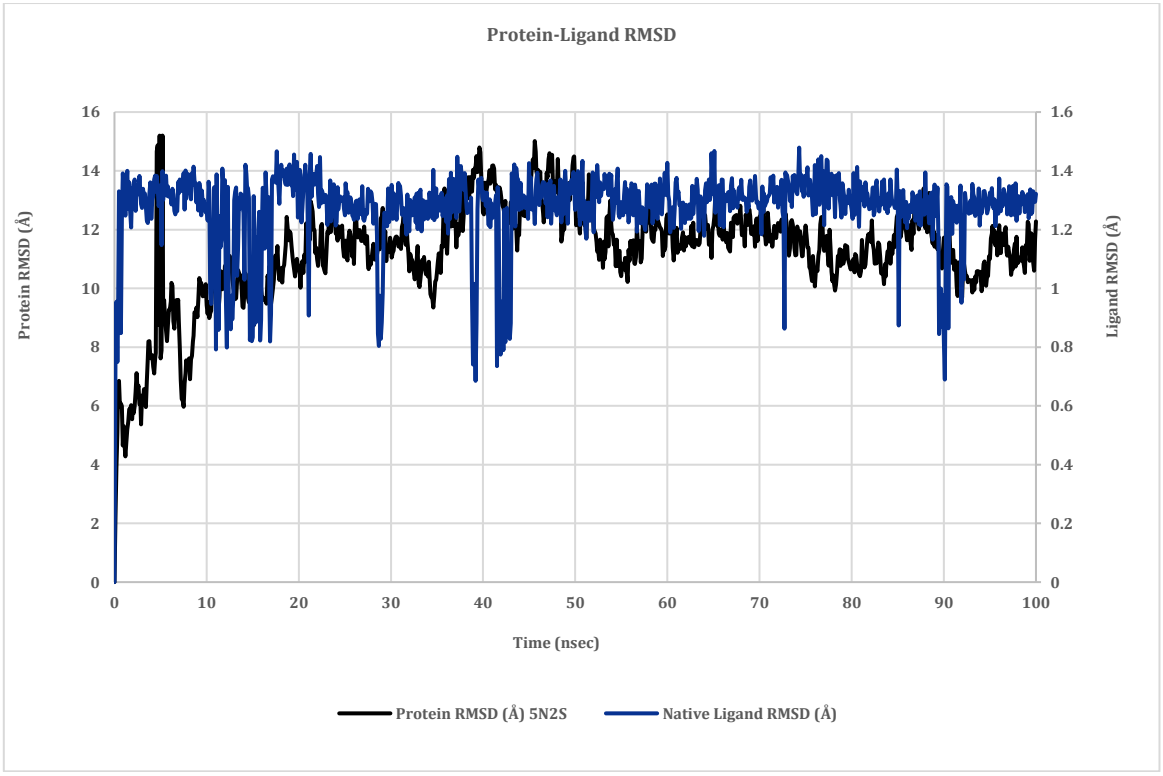

A

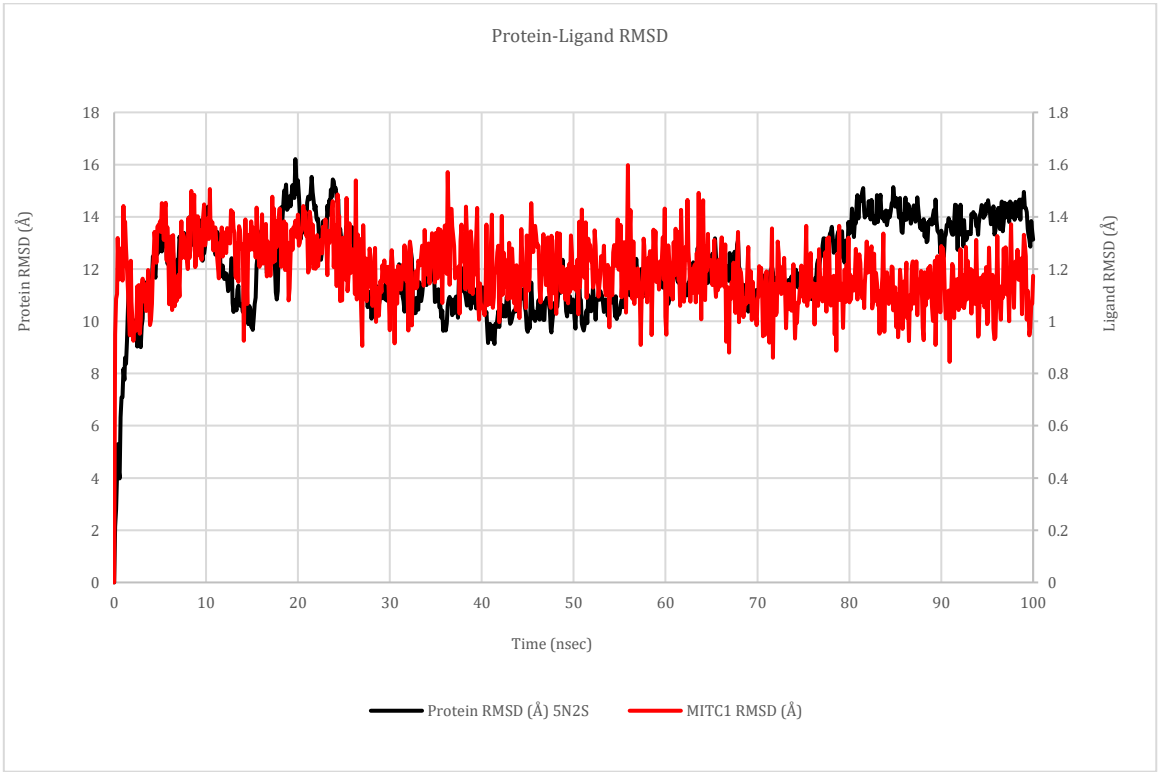

B

Fig. 5: RSMD of co-crystallized (A) and MITC-1 (B) ligands in complex with A_1R receptor during a 100 ns MD simulation period. RMSD of A_1R on the left Y-axis and the ligand RMSD profile aligned on the right X-axis

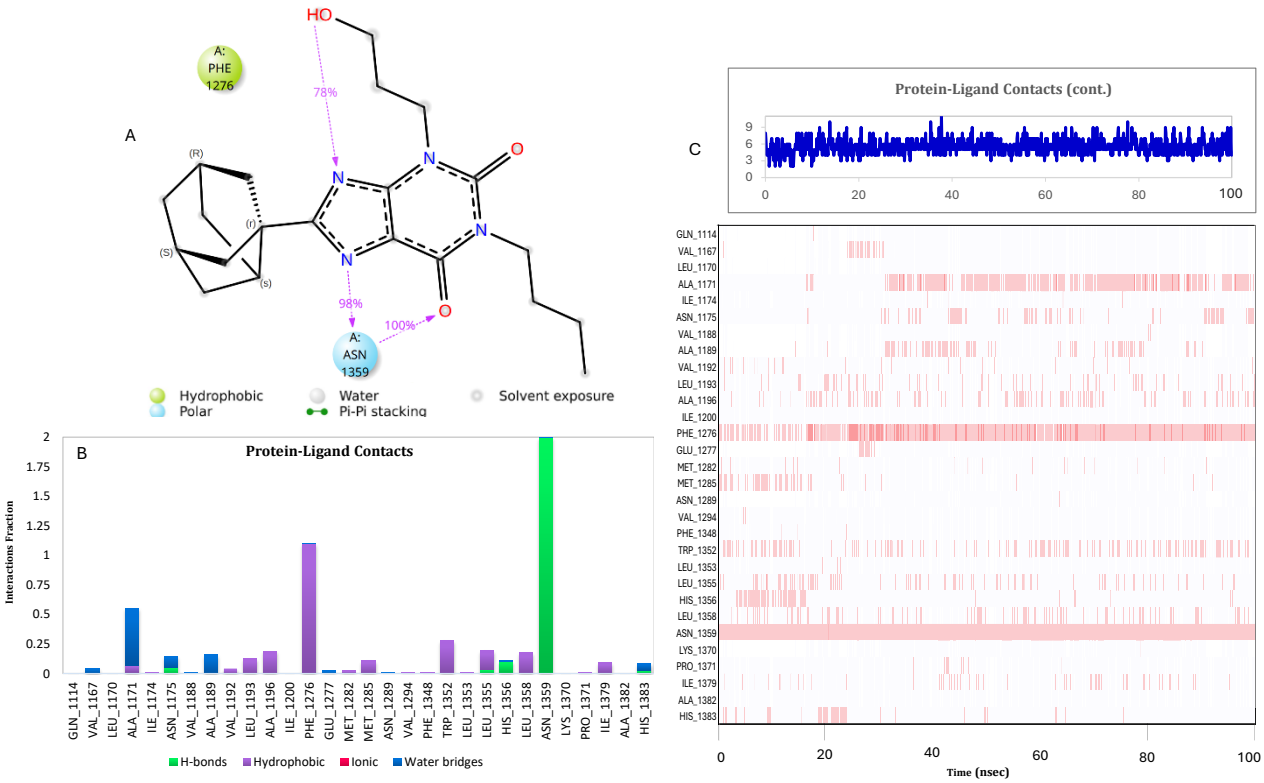

Fig. 6: (A) 2D atomic interactions of the co-crystallized ligand with A_1R were maintained for over 30% of the trajectory. (B) Stacked bar chart of interactions between the co-crystallized ligand and A_1R residues during the simulation. (C) Timeline of protein-ligand interactions, with the top panel showing total interactions and the bottom panel highlighting residue-specific interactions per frame. Dark orange indicates multiple interactions

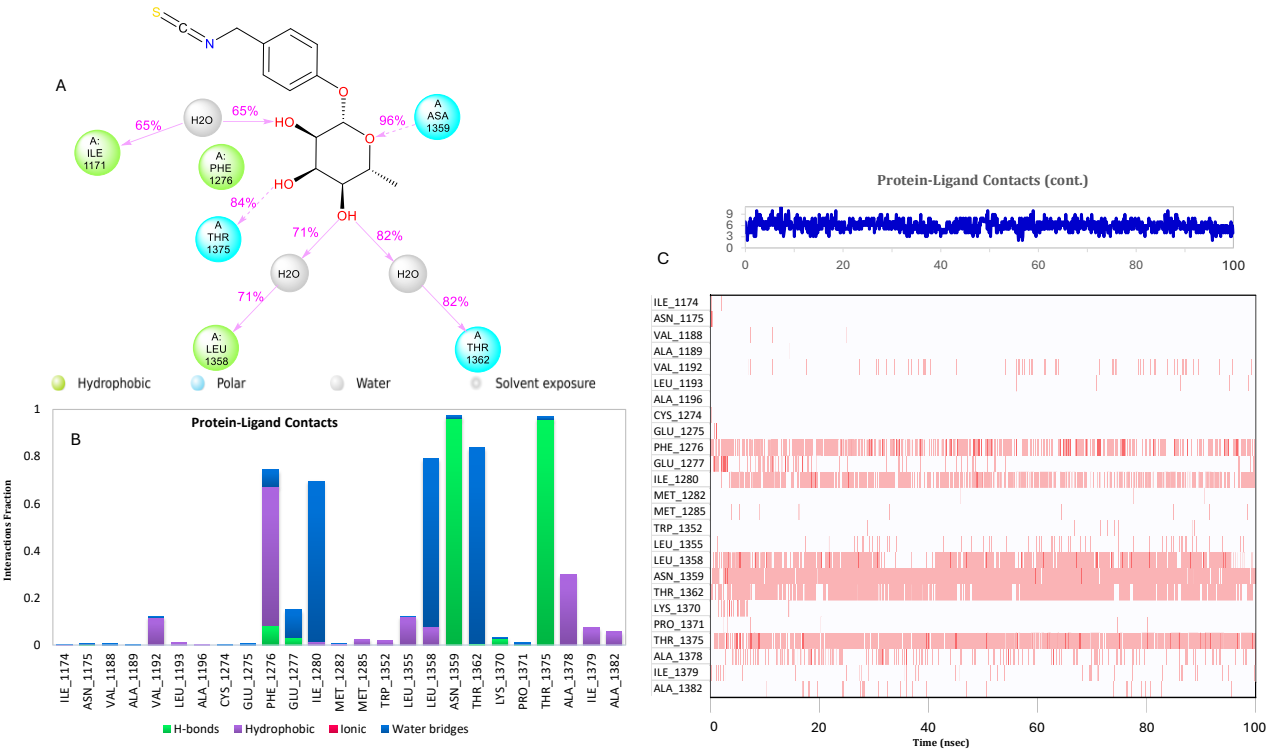

Fig. 7: (A) 2D atomic interactions of MITC-1 with A_1R were maintained for over 30% of the trajectory. (B) Stacked bar chart of interactions between MITC-1 and A_1R residues during the simulation. (C) Timeline of protein-ligand interactions, with the top panel showing total interactions and the bottom panel highlighting residue-specific interactions per frame. Dark orange indicates multiple interactions

3.4. ADEMT and drug-likeness

The evaluation of the drug-like and ADMET properties of the native ligand and MITCs using Maestro's QikProp module in Schrödinger provided comprehensive insights into their therapeutic potential. The predicted values were compared against the recommended ranges established from

95% of known drugs, as detailed in Table 4. All MITCs demonstrated favorable drug-likeness and ADMET properties within the normal range, closely aligning with these benchmarks. These findings suggest that the compounds have promising therapeutic potential and are likely to be safe and effective for treating various conditions, including heart failure.

Notably, the #Stars descriptor showed that all MITCs scored 0, indicating excellent compliance with drug-likeness criteria. The dipole moments for the MITCs ranged from 2.698 to 4.160, well within the recommended range (1–12.50), suggesting balanced polarity to support effective interactions with biological membranes and proteins. Moreover, compounds present low toxicity risks, as evidenced by QPlogHERG values that exceed the concern threshold (-5), signifying minimal cardiac toxicity associated with HERG K+ channel inhibition. Additionally, the reactive functional groups (#RtvFG) remain within acceptable limits, further underscoring their safety profile.

The predicted octanol-water partition coefficients (QPlogPo/w) ranged from 0.691 to 1.429, indicating moderate lipophilicity conducive to effective absorption and distribution. Aqueous solubility (QPlogS) values fall within the acceptable range (-6.5 to 0.5), demonstrating adequate solubility for the compounds. Binding affinity to human serum albumin (QPlogKhsa) values also lie within recommended limits, ensuring efficient plasma protein binding and distribution. Moreover, predicted human oral absorption percentages (78.330% to 83.343%) are high, suggesting strong bioavailability for all compounds. The comparable results between MITCs and the native ligand PSB36, known for its high affinity to A_1R, highlight their potential as effective treatment agents for heart failure and its associated complications. These findings lay a strong groundwork for advancing MITCs in the drug development process. However, further experimental validation is crucial to confirm these predictions and assess the compounds' efficacy and safety in clinical applications.

Table 4: The absorption, distribution, metabolism, excretion, and toxicity of MITCs prepared by QikProp

Descriptors	Recommended range	Native ligand	MITC-1	MITC-2	MITC-3	MITC-4
Mol_MW		386.493	311.352	353.389	353.389	353.389
#Stars	(0.0–5.0)	0	0	0	0	0
Dipole	(1–12.50)	8.047	3.136	4.16	2.698	3.606
SASA	(300–1000)	681.156	563.69	634.09	620.523	640.937
DonorHB	(0–6)	2	3	2	2	2
AccptHB	(2.0–20.0)	6.7	10.05	10.35	10.35	10.35
QPlogPo/w	(-2–6.5)	3.264	0.691	1.388	1.357	1.429
QPlogS	(-6.5–0.5)	-5.065	-2.6	-3.4	-3.193	-3.507
QPlogHERG	Concern below -5	-4.484	-4.758	-5.183	-4.898	-5.284
QPlogBB	(-3–1.2)	-1.133	-1.05	-1.118	-1.059	-1.116
QPlogKp	(-8.8–1.0)	-3.188	-2.912	-2.872	-2.893	-2.83
#Metab	(1–8)	1	4	3	3	3
QPlogKhsa	(-1.5–1.5)	0.364	-0.814	-0.66	-0.658	-0.655
%Human oral absorption	(<25% poor; >80% high)	95.772	78.33	82.732	82.738	83.343
CNS	(-2 inactive) (+2 active)	-2	-2	-2	-2	-2
#RtvFG	(0–2)	0	1	2	2	2

Heart failure (HF) is a complex syndrome where the heart fails to pump sufficient blood to meet the body's needs, resulting in symptoms such as fatigue, breathlessness, and fluid retention. A major complication of HF is its impact on kidney function, leading to cardiorenal syndrome, where heart and kidney dysfunctions exacerbate each other. Reduced cardiac output in HF decreases renal perfusion, causing sodium and water retention, worsening fluid overload, and increasing strain on the heart. Adenosine, through its receptors (A_1, A_{2A}, A_{2B}, and A_3), plays a crucial role in cardiovascular and renal regulation (Bahreyni et al., 2024; Gottlieb et al., 2011; Thai et al., 2024).

Activation of A_1R reduces cyclic adenosine monophosphate (cAMP) levels and protein kinase A (PKA) activity, decreasing calcium influx into cardiac cells. This cascade diminishes myocardial contractility and heart rate. Dysregulation of A_1R activity exacerbates HF progression by impairing cardiac output, contractility, and heart rate regulation (Chen et al., 2013; Gottlieb et al., 2011; Jacobson and Gao, 2006; Schenone et al., 2010; Thai et al., 2024). In the kidneys, A_1R activation promotes sodium reabsorption and reduces the glomerular filtration rate (GFR), further contributing to fluid retention and volume overload (Gottlieb et al., 2011; Hocher, 2010; Nguyen et al., 2023; Olayanju et al., 2024; Thai et al., 2024).

Drugs targeting A_1R have been investigated to improve cardiac function and manage HF symptoms. A_1R antagonists block adenosine binding, reversing its pathological effects by increasing cAMP and PKA activity, which enhances myocardial contractility and heart rate. Additionally, these antagonists exert diuretic effects by improving renal blood flow, increasing GFR, and promoting sodium excretion (natriuresis) without significantly affecting systemic hemodynamics. While these therapies show potential, clinical outcomes have been inconsistent, highlighting the need for further research (Chen et al., 2013; Gottlieb et al., 2011; Jacobson and Gao, 2006; Nguyen et al., 2023; Schenone et al., 2010; Thai et al., 2024).

Current studies support the cardiovascular protective effects of *Moringa oleifera* (Alia et al., 2022; Kamal et al., 2022). Methanolic root extracts have been shown to enhance myocyte contraction and oxygen delivery in a model of doxorubicin-induced HF. Seed extracts significantly reduced

myocardial infarction, improved cardiac contractility, and mitigated cardiac remodeling and fibrosis (Kamal et al., 2022). Leaf extracts also alleviated myocyte death, reduced cardiac injury markers, and decreased mortality in congestive heart failure (Kamal et al., 2022). Despite these promising findings, most studies have focused on crude extracts rather than purified compounds like MITC-1, leaving gaps in understanding the precise mechanisms of action.

Numerous studies have highlighted the significant cardiovascular protective effects of cruciferous Brassicas and their isothiocyanate derivatives. These compounds play a crucial role in combating atherosclerosis and other cardiovascular conditions by reducing inflammation and oxidative stress (Dinkova-Kostova and Kostov, 2012; Kamal et al., 2022). Sulforaphane is an isothiocyanate abundant in Brassicas vegetables, has been associated with decreased coronary artery disease risk in postmenopausal women, as well as improved lipid profiles by lowering LDL and total cholesterol and increasing HDL cholesterol. Sulforaphane exerts its effect via activation of Nrf2 (Nuclear factor erythroid 2-related factor 2), which is a key transcription factor that plays a critical role in cellular defense mechanisms, particularly against oxidative stress and inflammation. Nrf2 activation has significant implications for cardiovascular health (Bai et al., 2015). Allyl isothiocyanate, a natural isothiocyanate, has demonstrated cardiovascular protective effects through the activation of TRPA1 (Transient Receptor Potential Ankyrin 1). TRPA1 is a calcium-permeable ion channel that functions as a chemical sensor in sensory and cardiovascular tissues. Its activation offers protective benefits for cardiovascular health by reducing oxidative stress, modulating inflammation, and enhancing myocardial relaxation. This highlights allyl isothiocyanate as a potential therapeutic agent for age-related cardiac dysfunction and other conditions associated with oxidative damage and inflammation. While natural isothiocyanates have been studied for their effects on oxidative stress, inflammation, and activation of some proteins like TRPA1 and Nrf2, their role in inhibiting adenosine A_1 receptors (A_1R) for cardiovascular protection has not been documented in existence. Recent findings suggest that the cardiovascular protective effects of *Moringa oleifera* may be mediated through the antagonistic activity of MITC-1 on A_1R. This dual action could improve cardiac function and act as a diuretic to alleviate fluid overload, making it a promising candidate for heart failure treatment.

4. Conclusion

This study underscores the potential of *Moringa oleifera*-derived isothiocyanates, particularly MITC-1, as promising therapeutic agents for heart failure through their interaction with adenosine A_1 receptors (A_1R). Molecular docking and dynamics simulations revealed significant binding affinity and favorable interactions with the A_1R binding pocket, indicating that MITC-1 may function as a functional antagonist. Favorable ADMET properties further support MITC-1's viability as a drug candidate. By modulating A_1R activity, MITC-1 presents a novel approach to improving heart failure outcomes, warranting further investigation in preclinical and clinical settings to confirm its therapeutic efficacy and elucidate its mechanisms of action. Future research should include *in vitro* assays to evaluate A_1R antagonistic activity and effects on cAMP, as well as *ex vivo* models to examine its diuretic potential. Additionally, pharmacokinetic and safety studies are essential for advancing MITC-1 in drug development.

List of abbreviations

#Metab	Number of predicted metabolic reactions
#RtvFG	Number of reactive functional groups
#Stars	Number of ADMET property violations
A_1R	Adenosine A_1 receptor
AccptHB	Hydrogen bond acceptors
ADMET	Absorption, distribution, metabolism, excretion, and toxicity
ATC	Anatomical therapeutic chemical classification system
CHF	Congestive heart failure
CNS	Central nervous system (activity score)
cAMP	Cyclic adenosine monophosphate
DonorHB	Hydrogen bond donors
GFR	Glomerular filtration rate
GPCRs	G protein-coupled receptors
HERG	Human ether-à-go-go-related gene (potassium channel)
ITCs	Isothiocyanates
MD	Molecular dynamics
MITCs	*Moringa oleifera*-derived isothiocyanates
Mol_MW	Molecular weight
NPT	Isothermal–isobaric ensemble (constant N, P, T)
Nrf2	Nuclear factor erythroid 2–related factor 2
OPLS	Optimized potentials for liquid simulations
PDB	Protein Data Bank
PKA	Protein kinase A
PSB36	1-butyl-3-(3-hydroxypropyl)-8-(3-noradamantyl)xanthine
QPlogBB	Predicted brain/blood partition coefficient
QPlogHERG	Predicted HERG K^+ channel inhibition
QPlogKhsa	Predicted binding to human serum albumin
QPlogKp	Predicted skin permeability
QPlogPo/w	Predicted octanol/water partition coefficient
QPlogS	Predicted aqueous solubility
RMSD	Root mean square deviation
SASA	Solvent accessible surface area
TIP3P	Transferable intermolecular potential with 3 points
TRPA1	Transient receptor potential ankyrin 1
VdW	Van der Waals
XP	Extra precision (docking mode in Glide)

Funding

This work was funded by the University of Jeddah, Jeddah, Saudi Arabia, under Grant No. (UJ-23-RSP-7). The author thanks the University of Jeddah for their technical and financial support.

Compliance with ethical standards

Conflict of interest

The author(s) declared no potential conflicts of interest with respect to the research, authorship, and/or publication of this article.

References

Alia F, Putri M, Anggraeni N, and Syamsunarno MRAA (2022). The potency of *Moringa oleifera* Lam: As protective agent in cardiac damage and vascular dysfunction. Frontiers in Pharmacology, 12: 724439. https://doi.org/10.3389/fphar.2021.724439 **PMid:35140601 PMCid:PMC8818947**

Bahreyni A, Saeedi N, Al-Asady AM, Soleimani A, Ghorbani E, Khazaei M, Alaei M, Hanaei R, Ryzhikov M, Avan A, and Hassanian SM (2024). Therapeutic potency of A_1 adenosine receptor antagonists in the treatment of cardiovascular diseases, current status and perspectives. Molecular Biology Reports, 51: 358. https://doi.org/10.1007/s11033-024-09246-6 **PMid:38400849**

Bai Y, Wang X, Zhao S, Ma C, Cui J, and Zheng Y (2015). Sulforaphane protects against cardiovascular disease via Nrf2 activation. Oxidative Medicine and Cellular Longevity, 2015: 407580. https://doi.org/10.1155/2015/407580 **PMid:26583056 PMCid:PMC4637098**

Basheer R, Strecker RE, Thakkar MM, and McCarley RW (2004). Adenosine and sleep–wake regulation. Progress in Neurobiology, 73(6): 379-396. https://doi.org/10.1016/j.pneurobio.2004.06.004 **PMid:15313333**

Borea PA, Gessi S, Merighi S, Vincenzi F, and Varani K (2018). Pharmacology of adenosine receptors: The state of the art. Physiological Reviews, 98(3): 1591-1625. https://doi.org/10.1152/physrev.00049.2017 **PMid:29848236**

Chen JF, Eltzschig HK, and Fredholm BB (2013). Adenosine receptors as drug targets—what are the challenges? Nature Reviews Drug Discovery, 12: 265-286. https://doi.org/10.1038/nrd3955 **PMid:23535933 PMCid:PMC3930074**

Cheng RK, Segala E, Robertson N, Deflorian F, Doré AS, Errey JC, Fiez-Vandal C, Marshall FH, and Cooke RM (2017). Structures of human A_1 and A_{2A} adenosine receptors with xanthines reveal determinants of selectivity. Structure, 25(8): 1275-1285.e4. https://doi.org/10.1016/j.str.2017.06.012 **PMid:28712806**

Dhalla AK, Shryock JC, Shreeniwas R, and Belardinelli L (2003). Pharmacology and therapeutic applications of A_1 adenosine receptor ligands. Current Topics in Medicinal Chemistry, 3(4): 369-385. https://doi.org/10.2174/1568026033392246 **PMid:12570756**

Dinkova-Kostova AT and Kostov RV (2012). Glucosinolates and isothiocyanates in health and disease. Trends in Molecular Medicine, 18(6): 337-347. https://doi.org/10.1016/j.molmed.2012.04.003 **PMid:22578879**

Dunkel M, Günther S, Ahmed J, Wittig B, and Preissner R (2008). SuperPred: Drug classification and target prediction. Nucleic Acids Research, 36(suppl_2): W55-W59. https://doi.org/10.1093/nar/gkn307 **PMid:18499712 PMCid:PMC2447784**

Giacoppo S, Galuppo M, Montaut S, Iori R, Rollin P, Bramanti P, and Mazzon E (2015). An overview on neuroprotective effects of isothiocyanates for the treatment of neurodegenerative diseases. Fitoterapia, 106: 12-21. https://doi.org/10.1016/j.fitote.2015.08.001 **PMid:26254971**

Gottlieb SS, Ticho B, Deykin A, Abraham WT, DeNofrio D, Russell SD, Chapman D, Smith W, Goldman S, and Thomas I (2011). Effects of BG9928, an adenosine A_1 receptor antagonist, in patients with congestive heart failure. The Journal of Clinical Pharmacology, 51: 899-907. https://doi.org/10.1177/0091270010375957 **PMid:20926754**

Hocher B (2010). Adenosine A_1 receptor antagonists in clinical research and development. Kidney International, 78(5): 438-445. https://doi.org/10.1038/ki.2010.204 **PMid:20592713**

Ioakimidis L, Thoukydidis L, Mirza A, Naeem S, and Reynisson J (2008). Benchmarking the reliability of QikProp: Correlation between experimental and predicted values. QSAR and Combinatorial Science, 27: 445-456. https://doi.org/10.1002/qsar.200730051

Jacobson KA and Gao ZG (2006). Adenosine receptors as therapeutic targets. Nature Reviews Drug Discovery, 5: 247-264. https://doi.org/10.1038/nrd1983 **PMid:16518376 PMCid:PMC3463109**

Jaja-Chimedza A, Graf BL, Simmler C, Kim Y, Kuhn P, Pauli GF, and Raskin I (2017). Biochemical characterization and anti-inflammatory properties of an isothiocyanate-enriched moringa (*Moringa oleifera*) seed extract. PLOS ONE, 12(8): e0182658. https://doi.org/10.1371/journal.pone.0182658 **PMid:28792522 PMCid:PMC5549737**

Kamal RM, Abdull Razis AF, Mohd Sukri NS, Perimal EK, Ahmad H, Patrick R, Djedaini-Pilard F, Mazzon E, and Rigaud S (2022). Beneficial health effects of glucosinolates-derived isothiocyanates on cardiovascular and neurodegenerative diseases. Molecules, 27(3): 624. https://doi.org/10.3390/molecules27030624 **PMid:35163897 PMCid:PMC8838317**

Lopez-Rodriguez NA, Gaytán-Martínez M, de la Luz Reyes-Vega M, and Loarca-Piña G (2020). Glucosinolates and isothiocyanates from *Moringa oleifera*: Chemical and biological approaches. Plant Foods for Human Nutrition, 75: 447-457. https://doi.org/10.1007/s11130-020-00851-x **PMid:32909179**

Mastuo T, Miyata Y, Yuno T, Mukae Y, Otsubo A, Mitsunari K, Ohba K, and Sakai H (2020). Molecular mechanisms of the anti-cancer effects of isothiocyanates from cruciferous vegetables in bladder cancer. Molecules, 25(3): 575. https://doi.org/10.3390/molecules25030575 **PMid:32013065 PMCid:PMC7037050**

Na G, He C, Zhang S, Tian S, Bao Y, and Shan Y (2023). Dietary isothiocyanates: Novel insights into the potential for cancer prevention and therapy. International Journal of Molecular Sciences, 24(3): 1962. https://doi.org/10.3390/ijms24031962 **PMid:36768284 PMCid:PMC9916827**

Nguyen AT, Tran QL, Baltos JA, McNeill SM, Nguyen DT, and May LT (2023). Small molecule allosteric modulation of the adenosine A_1 receptor. Frontiers in Endocrinology, 14: 1184360. https://doi.org/10.3389/fendo.2023.1184360 **PMid:37435481 PMCid:PMC10331460**

Olayanju JB, Bozic D, Naidoo U, and Sadik OA (2024). A comparative review of key isothiocyanates and their health benefits. Nutrients, 16(6): 757. https://doi.org/10.3390/nu16060757 **PMid:38542669 PMCid:PMC10974736**

Sahin N, Orhan C, Erten F, Tuzcu M, Defo Deeh PB, Ozercan IH, Juturu V, and Kazim S (2019). Effects of allyl isothiocyanate on insulin resistance, oxidative stress status, and transcription factors in high-fat diet/streptozotocin-induced type 2 diabetes

mellitus in rats. Journal of Biochemical and Molecular Toxicology, 33: e22328. https://doi.org/10.1002/jbt.22328 **PMid:30927557**

Schenone S, Brullo C, Musumeci F, Bruno O, and Botta M (2010). A_1 receptors ligands: Past, present and future trends. Current Topics in Medicinal Chemistry, 10(9): 878-901. https://doi.org/10.2174/156802610791268729 **PMid:20370661**

Schrödinger LLC (2024a). Schrödinger Release 2024-3: Glide. Schrödinger, LLC, New York, USA.

Schrödinger LLC (2024b). Schrödinger Release 2024-3: LigPrep. Schrödinger, LLC, New York, USA.

Schrödinger LLC (2024c). Schrödinger Release 2024-3: Protein Preparation Wizard. Schrödinger, LLC, New York, USA.

Schrödinger LLC (2024d). Schrödinger Release 2024-3: QikProp. Schrödinger, LLC, New York, USA.

Sheth S, Brito R, Mukherjea D, Rybak LP, and Ramkumar V (2014). Adenosine receptors: Expression, function and regulation. International Journal of Molecular Sciences, 15(2): 2024-2052. https://doi.org/10.3390/ijms15022024 **PMid:24477263 PMCid:PMC3958836**

Tawfik HE, Schnermann J, Oldenburg PJ, and Mustafa SJ (2005). Role of A_1 adenosine receptors in regulation of vascular tone. American Journal of Physiology-Heart and Circulatory Physiology, 288(3): H1411-H1416. https://doi.org/10.1152/ajpheart.00684.2004 **PMid:15539423**

Thai BS, Chia LY, Nguyen AT, Qin C, Ritchie RH, Hutchinson DS, Kompa A, White PJ, and May LT (2024). Targeting G protein-coupled receptors for heart failure treatment. British Journal of Pharmacology, 181(14): 2270-2286. https://doi.org/10.1111/bph.16099 **PMid:37095602**

Vallon V, Miracle C, and Thomson S (2008). Adenosine and kidney function: Potential implications in patients with heart failure. European Journal of Heart Failure, 10: 176-187. https://doi.org/10.1016/j.ejheart.2008.01.010 **PMid:18242127 PMCid:PMC3151609**

Vincenzi F, Pasquini S, Contri C, Cappello M, Nigro M, Travagli A, Merighi S, Gessi S, Borea PA, and Varani K (2023). Pharmacology of adenosine receptors: Recent advancements. Biomolecules, 13(9): 1387. https://doi.org/10.3390/biom13091387 **PMid:37759787 PMCid:PMC10527030**

Waterman C, Cheng DM, Rojas-Silva P, Poulev A, Dreifus J, Lila MA, and Raskin I (2014). Stable, water extractable isothiocyanates from *Moringa oleifera* leaves attenuate inflammation *in vitro*. Phytochemistry, 103: 114-122. https://doi.org/10.1016/j.phytochem.2014.03.028 **PMid:24731259 PMCid:PMC4071966**